Energy 283 (2023) 129163

Contents lists available at ScienceDirect

Energy

journal homepage: www.elsevier.com/locate/energy

Development of a spray-ejector condenser for the use in a negative CO_2 emission gas power plant

Paweł Madejski [a,*], Krzysztof Banasiak [b], Paweł Ziółkowski [c], Dariusz Mikielewicz [c], Jarosław Mikielewicz [d], Tomasz Kuś [a], Michał Karch [a], Piotr Michalak [a], Milad Amiri [c], Paweł Dąbrowski [c], Kamil Stasiak [c], Navaneethan Subramanian [a], Tomasz Ochrymiuk [d]

[a] AGH University of Science and Technology, Faculty of Mechanical Engineering and Robotics, Department of Power Systems and Environmental Protection Facilities, Kraków, Poland
[b] SINTEF Energy, Trondheim, Norway
[c] Gdańsk University of Technology, Faculty of Mechanical Engineering and Ship Technology, Gdańsk, Poland
[d] Institute of Fluid Flow Machinery, Polish Academy of Sciences, Energy Conversion Department, Gdańsk, Poland

ARTICLE INFO

Handling Editor: Wojciech Stanek

Keywords:
Two-phase ejector
Negative CO_2 gas power plant
CO_2 capture
Mathematical modeling
Spray-ejector condenser (SEC)
CFD modeling

ABSTRACT

One promising solution for developing low-emission power technologies is using gaseous fuel combustion in pure oxygen when the exhaust gas mixture is composed of H_2O and CO_2, and where CO_2 is separated after steam condensation. The paper presents the results of computational analyses providing to the Spray-Ejector Condenser (SEC) development, which is one of the crucial components of the negative CO_2 gas power plant (nCO_2PP) cycle development. The proposed design of the ejector-condenser to ensure the high effectivity of vapor condensation and CO_2 compression with preparation to separation, ready for application in gas power cycle, is a novelty of this research. Different computational techniques leading to the development and better understating of ejector operation were applied. The main operating conditions in the characteristic connected with the developed nCO2pp cycle points were investigated to evaluate the impact of the operating conditions on SEC performances. The amount of motive water needed for the cooling purpose is susceptible to the inlet water pressure and temperature and strongly affects the generated pressure of the suction stream. The preliminary results confirm that the SEC's basic design and geometrical dimensions can be applied in the negative CO_2 power plant cycle. Results from CFD modeling give the possibility to investigate the turbulent flow of water/steam/CO_2 mixture together with the condensation process occurring at this same time. It is found that the average droplet diameter and motive water supplying method significantly effects the condensation intensity. The further direction of the presented computational research activities and results is to test various designs of Spray-Ejector Condensers that will enable the evaluation of the direct contact condensation process and develop the final geometrical design.

1. Introduction

In surface condensers, direct contact between exhaust vapor (mainly steam) and fluid (mainly water) doesn't exist. The vapor (steam) passes over the outer surface of tubes when a cooling fluid (water) is supplied through the tubes. The temperature of condensed steam depends on the pressure inside the surface condenser (saturation temperature at condenser pressure). The cooling water temperature increases, which depends on the mass flow rate of the cooling water [1–4]. Direct Contact Condensers have been widely used for over a century in various industrial applications such as petroleum and chemical engineering, desalination installations, and power plants [5]. Due to the pump's loss of condensate and high power requirement, these condensers are rarely used in modern steam power plants. Direct Contact Condensers are divided into spray-type, film-type, and bubbling types [6,7]. In the first solution, the sprayed liquid phase flows downwards and is in contact with flowing upwards gas. In the second case, both phases flow counter currently. In the latter solution, the bubbling gas phase passes through the liquid layer. Furthermore, spray condensers can exist with constant pressure or constant area jet ejectors.

One of the proposed types of Direct Contact Condensers is a Spray-Ejector Condenser, a combination of an ejector providing pressure lift

* Corresponding author.
E-mail address: pawel.madejski@agh.edu.pl (P. Madejski).

https://doi.org/10.1016/j.energy.2023.129163
Received 3 April 2023; Received in revised form 20 September 2023; Accepted 21 September 2023
Available online 22 September 2023
0360-5442/© 2023 The Authors. Published by Elsevier Ltd. This is an open access article under the CC BY-NC license (http://creativecommons.org/licenses/by-nc/4.0/).

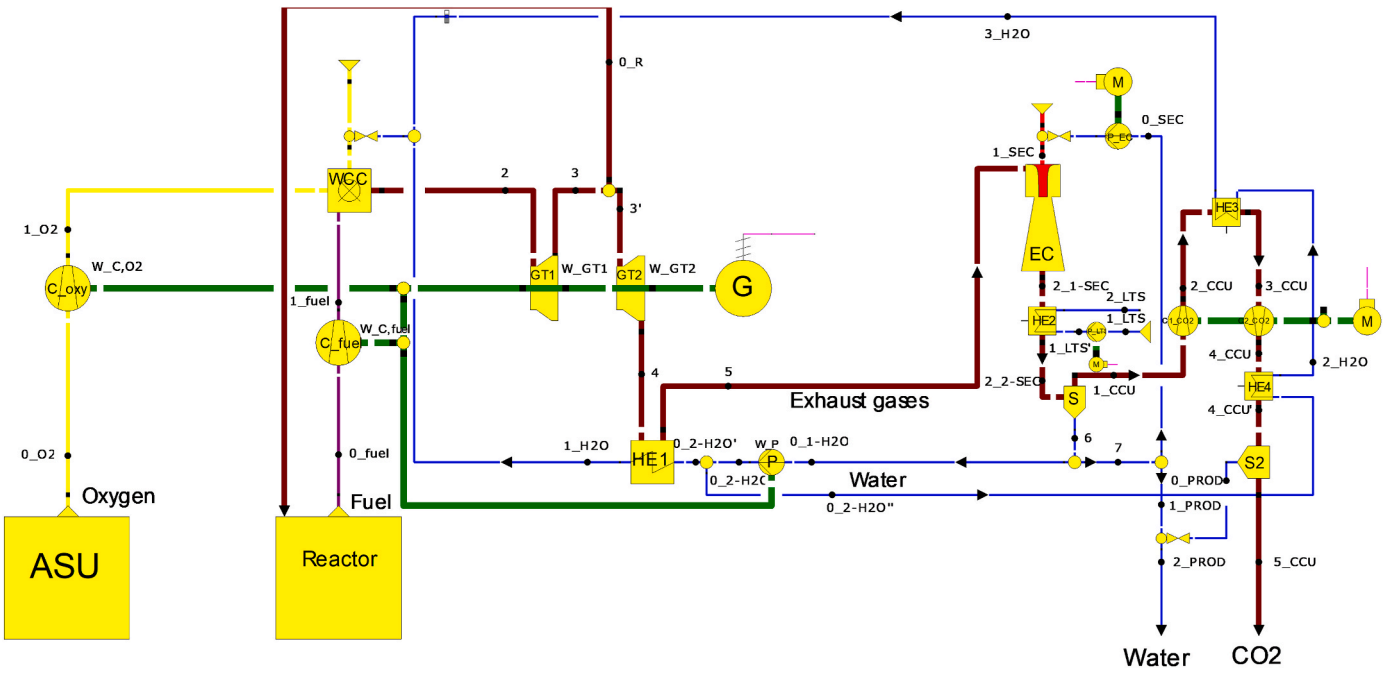

Fig. 1. Process flow diagram of a negative CO_2 emission gas cycle. C_{oxy} – oxygen compressor; C_{fuel} – gas fuel compressor; WCC – Wet Combustion Chamber; GT1, GT2 – gas turbines; G – electricity generator; EC – Spray-Ejector Condenser (Ejector Condenser); HE1, HE2, HE3, HE4 – heat exchangers, P – water pump; P_{EC} – SEC water pump; M – motor; S – separator; $C1_{CO2}$, $C2_{CO2}$ – CO_2 compressors.

and a condenser allowing gas condensation. The spray-ejector condenser belongs to the group of direct-contact heat exchangers, which can be smaller, cheaper, and have a simpler construction than the surface, shell, or tube heat exchangers of the same capacity and can operate in evaporation or condensation mode [6]. Due to direct contact with process fluids, its construction is simpler and more corrosion resistant [8], less expensive [9], easier to maintain, and simpler in operation [10]. Direct contact condensers can be widely used in oxy-fuel combustion capture systems, but high water vapor content in the flue gas requires rigorous sizing procedures for the condenser design [11]. Desuperheater vessels have attracted attention as a domestic provision involving steam-induced direct contact condensation. The experimental investigation of pressurized pulsating steam injected co-currently with slow-moving water in a cylindrical vessel is presented by Ghazwani et al. [12]. Sokolow and Zinger [13] investigated experimentally water-driven two-phase flow ejectors as the promising solution for application as water jet heaters. The intensity of the heat transfer process from steam to water when the phases are in direct contact is much higher than the heat transfer intensity in surface heat exchangers. The simpler and smaller construction of jet heaters is an advantage. The phenomena that improve the exchange of mass, momentum, and energy in Spray-Ejector Condenser start from the supply nozzle, where the primary fluid can be appropriately applied and broken up into tens to thousands of droplets of dimensions resulting from the geometry of a nozzle, supply parameters, and geometry of the channel appropriate to the parameters of the SEC device. Consequently, localized flow discontinuities in the integrity of the jet can form at the edges, i.e. voids are created at pressures well below the saturation pressure of the fluid. In doing so, the disintegration of the liquid into droplets occurs, and the conversion of the internal energy and enthalpy of the liquid stream into kinetic energy and surface tension energy can then take place as a result of the destruction of the continuous media. The stream of primary fluid thus leaves the nozzle cross-section in a discrete form with a huge number of droplets having a velocity that depends on the nozzle shape. Under extreme conditions, the dispersed jet of motive fluid can behave in principle as a free stream, i.e. not interacting with the surrounding gaseous stream drawn into the nozzle. However, a number of small-scale phenomena occur in reality [14–17]. These phenomena affect the global characteristics of the device, which will be obtained through experimental and theoretical analysis. The direct condensation of steam from a mixture of steam and inert gas (CO_2) occurs on droplets formed from the decomposition of the cooling water jet, where the water flow and the steam-gas mixture do not form a supercritical flow. When a supercritical flow is formed from a mixture of steam and gas and cooling water, a shock wave is formed, condensing the steam under conditions of thermodynamic non-equilibrium. Such condensation can arise without the cooling water cooling the mixture. Such a case occurs in the last stages of steam turbines. This paper presents the first case of a subcritical flow of a mixture of steam and inert gas, and cooling water and the study aims to introduce the results of numerical calculations for developing the Spray-Ejector Condenser as an application for the negative CO_2 gas power plant cycle [18].

The negative CO_2 emission has gained special significance in recent years because of the rising importance of developing new efficient energy technologies. Ziółkowski et al. [19] presented the developed cycle of a negative CO_2 emission power plant using gasified sewage sludge as a main fuel. The results of a negative CO_2 emission power plant modeling, using gasified sewage sludge as a main fuel, with a turbine cooperating with a Spray-Ejector Condenser (SEC) are presented in detail in Refs. [20,21]. Simulations performed with three different tools (Aspen Plus, Aspen Hysys, and Ebsilon) showed similar results for a turbine gross efficiency and output power. The main sources of exergy destruction in the presented cycle (Fig. 1) are the wet combustion chamber and the Spray-Ejector Condenser [21,22]. It can be noted that the mass flow rate of injected cooling water is quite large and can reach about 200 times that of the flue gas. To avoid the efficiency reduction of the presented cycle (Fig. 1), one of the research activities has to be focused on developing the most effective design of the Spray-Ejector Condenser.

The basic design and main operating conditions of the proposed Spray-Ejector Condenser can be developed with the use of the numerical simulations, CFD modeling and analytical modeling results. One approach is using an upgraded model of the previously developed 1D ejector model for transcritical CO_2 ejectors in refrigeration applications [24]. Despite one-dimensionality, due to expected subcritical velocities

MOST WIEDZY Downloaded from mostwiedzy.pl

throughout SEC flow path and no shock wave propagation, it is expected the model should catch most of the governing phenomena here, being able to deliver estimates of flow profiles for given geometry and boundary conditions. The second modeling approach is to develop a two-dimensional numerical model of SEC, using CFD modeling and software. In CFD models, mainly three different approaches are used for multiphase problem modeling: Mixture Multiphase Model (MMP), Volume of Fluid (VOF), and Eulerian Multiphase Model (EMP) [25]. To modeling the condensation process, Spalding Evaporation/Condensation model for Mixture Multiphase Model (MMP) can be used in the developed CFD model. The main idea of this model is to express the steady convective mass transfer phenomena using the Ohm's law relation [26]. Another approach to condensation process modeling using CFD methods is the Boiling/Condensation model, which is also available where the Mixture Multiphase Model (MMP) is used.

This paper presents the computational modeling results of a mixture of steam and inert gas and cooling water subcritical flow. The study aims to introduce the results of numerical calculations for developing the Spray-Ejector Condenser as an application for the negative CO_2 gas power plant cycle. The using of direct contact condensers can be very profitable but to the best of the authors' knowledge, the combination of an ejector and condenser for application in negative gas power plants to allow CO_2 separation has not been developed. The complex phenomena's occurring inside Spray-Ejector Condenser as turbulent multiphase flow, convective heat transfer, vapor condensation in the presence of inert gas requires the development of advanced numerical and analytical models, to fully investigate the ejector condenser performance and propose a geometrical model for considering operating conditions. Moreover, the diversity of applied tools provides a chance for a deep analysis of phenomena inside the ejector, which are still not fully understood because of their complexity. The necessary simulations were performed in the first step to verify the possibilities of SEC application and evaluate the nominal conditions of the presented solution. Then, using calculated values, more detailed models were developed, allowing an opportunity to analyze the physical phenomena inside SEC and their impact on the performances of the developed device. Within the project framework, the computational results' experimental validation is planned with a sign of a prototype test-rig installation. The studies [27,28] include a description of the concept, schematics, operating ranges, proposals for acquisition and monitoring of operating parameters, and basic assumptions for implementing the Spray-Ejector Condenser installation. The selected crucial issues to carrying out the experimental research in the SEC system were investigated. The presented results are directly connected with ongoing research on prototype research of the Negative CO_2 emission Gas Power Plant [18].

2. Negative CO_2 emission gas power plant concept

The presented cycle (Fig. 1) is based on combustion in an oxygen atmosphere, giving mainly CO_2 and water vapor. The CO_2 capture method uses a direct-contact heat exchanger (Spray-Ejector Condenser-SEC) to condense steam and thereby separate CO_2. This method and installation of CCS (Carbon Capture and Storage) reduce CO_2 emission. When the gas fuel comes from the gasification process of biomass or sewage sludge, as in the presented idea, the CO_2 emission is reduced below zero level, and the case of negative CO_2 emission gas power plant is achieved.

The cycle based on the oxy-combustion gas turbine cycle with the CO_2 capture installation components is presented in Fig. 1. The flows of gas fuel (0^{fuel}) and oxygen (0^{O2}) are compressed in compressors C_{oxy} and C_{fuel} from the inlet pressures to combustor injection pressure and fed (1^{fuel} and 1^{O2}) to the *WCC*. The inlet liquid water flow ($0^{1\text{-}H2O}$) is pumped (pump *P*), heated in a recuperator (heat exchanger *HE1*) and then injected (1^{H2O}) to the *WCC*. The fuel is burned with oxygen. Water is injected and evaporated to keep the temperature appropriate for the strength of the materials. The flue gas (*2*) is expanded trough gas

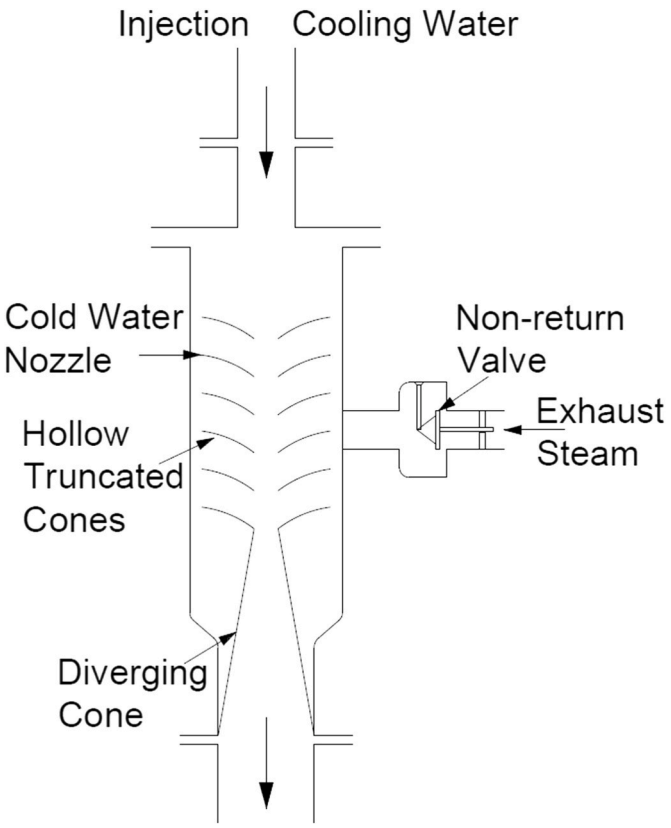

Fig. 2. Ejector-flow jet-type condenser.

turbines *GT1* and *GT2*, and then used to heat the incoming water (*HE1*). The gas turbines power the compressors, a pump and a generator *G*. Assuming complete combustion with the stoichiometric air, the flue gas (*2* to *5*) consists of H_2O and CO_2. The exhaust gases at the *GT2* outlet (*5*) are ducted to the Spray-Ejector Condenser (*SEC*), whereby the steam is condensed by direct contact with the cold inlet water (1^{SEC}) delivered by the water pump (*PEC*). The further step is cooling the mixture of water/CO_2 ($2^{1\text{-}SEC}$) by heat exchange with a low-temperature cooling medium (Streams 1^{LTS} to 2^{LTS}) in heat exchanger *HE2*. Here ($2^{2\text{-}SEC}$), a substantial part of the H_2O condenses to liquid, which is separated (*6*) in a separator (*S*) and directed out of the system (1^{PROD}) or re-used for injection to the *SEC* or the *WCC* and for cooling (*HE4*, *HE3*). The remaining CO_2 rich gas (1^{CCU}) is compressed ($C1^{CO2}$, $C2^{CO2}$) and cooled (*HE3*, *HE4*) before it is removed beyond the system boundary (5^{CCU}). Electric motor, *M*, runs the pump *PEC* and the compressors $C1_{CO2}$, $C2_{CO2}$. The exhaust gases at the gas turbine (*GT2*) outlet compose of steam (H_2O) and carbon dioxide (CO_2). The mass share depends on the combustion process inside the WCC, and the exhaust gas temperature depends on the conditions of *HE1*. The exhaust gas pressure at the inlet to the ejector condenser (*SEC*) results from SEC operation, and low pressure at the SEC inlet can be controlled by the cooling water (motive water) mass flow rate. Reducing the pressure of the gas turbine outlet (*SEC* inlet) increases the cycle's power production and overall energy and exergy efficiency. Energy and exergy analyses [22,23] show that the increasing pressure and temperature of exhaust gases at the SEC inlet increases the exergy destruction, reducing cycle efficiency and output power. In specific cycle operating conditions, the exergy distribution of SEC can vary with ambient conditions, where the exhaust gas pressure depends on the injected water to the WCC. The exergy destruction in SEC part for higher ambient temperature is more significant.

Considering all presented conditions, developing a spray-ejector condenser needs a comprehensive analysis of thermodynamic properties during cycle operation, multiphase fluid flow characteristics inside

MOST WIEDZY Downloaded from mostwiedzy.pl

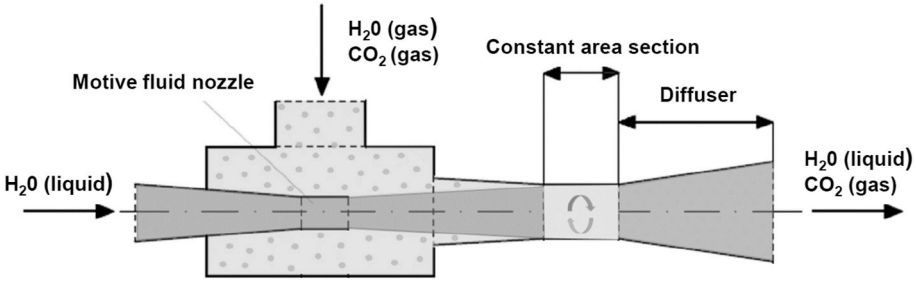

Fig. 3. General scheme of the ejector condenser principles operation.

the ejector geometrical part, and advanced heat transfer analysis during direct contact condensation of vapor in the presence of non-condensable CO_2 gas. These research activities should be done both numerically and experimentally.

3. Spray-ejector condenser for nCO2pp cycle

In jet-type condensers, the exhaust steam and water come in direct contact. The condensate temperature is the same as that of cooling water leaving the condenser. The cooling water is sprayed into the exhaust steam to start a rapid condensation. Heat exchange occurs by direct contact between steam and water. If the cooling water is not pure and free from harmful impurities, then the condensate cannot be reused as feed water. The exhaust steam and cooling water mix in hollow truncated cones in an ejector flow jet condenser (Fig. 2). Due to this decreased pressure, exhaust steam and associated air are drawn through the truncated cones, finally leading to the diverging cone. In the diverging cone, a portion of kinetic energy is converted into pressure energy which is more than the atmospheric, so that condensate consisting of condensed steam, cooling water, and air is discharged into the hot well. The exhaust steam inlet is provided with a non-return valve which does not allow the water from the hot well to rush back to the engine in case of cooling water supply to the condenser.

The name Spray-Ejector Condenser reflects the processes that were assumed to help realize the condensation of vapor and compression of CO_2 with preparation for separation. The first part "Spray," is related to the case following the phenomenon of the breakup of water leaving the nozzle. The second part "Ejector," means that to a large extent, the device has the shape and function of a water-gas jet, and the last part, "Condenser," refers to the device's main role is the condensation of steam. A schematic view of a Spray-Ejector Condenser is shown in Fig. 3. The cooling water enters the condenser and is discharged in the motive nozzle, where the potential energy is converted into kinetic energy, and thus a low-pressure area is created. The exhaust gases (steam and CO_2) enter the condenser and condense through the mixing section with cooling water; thus, the further vacuum increases. After passing through the mixing section, the mixture passes through the divergent nozzle. When it passes through the divergent nozzle, the kinetic energy of condensate reconverts into potential energy. Thus, higher pressure than the atmospheric pressure is obtained, which forces the condensate to the hot ambient. Therefore, in this condenser, no air extraction pump is required.

3.1. Conditions of spray-ejector condenser operation

The presented approach of the Spray-Ejector Condenser and with physical phenomena background make the Spray-Ejector Condenser (SEC) the preferred device for nCO_2PP cycles with CO_2 capture. In the case of the nCO2PP thermodynamic cycle, it can speak of a three-component ejector, as the steam is mixed with CO_2. The Spray-Ejector Condenser (SEC) is a device in which the liquid is used for compression, partial (or complete) condensation, and pumping of the gaseous mixture of steam and CO_2. In the presented case, the driving fluid is circulating water at a pressure of about 8 bar and a temperature of 15 °C. The gas is a binary mixture of water vapor and carbon dioxide from the turbine's low-pressure part. In contrast (to blowers and compressors), the main feature of this device is that it lacks the metal moving surfaces on which the medium usually acquires work, which is subsequently used for compression and kinetic energy [29]. The transfer of kinetic energy carried by the atomized water to the aspirated gas is a complex phenomenon in which various mechanisms are present. This process continues in the mixing section, which - having a constant cross-section - neither accelerates nor slows down the mixing phenomena of the two streams. Its length is most often determined experimentally and chosen so that the phenomena have time to equalize the driving potentials - hence it is usually assumed that the mixture stream leaving the mixing chamber should be homogeneous. In the case of a Spray-Ejector Condenser, there should be no homogenization with CO_2, so that the gas is precipitated from the liquid in the separator, e.g. using centrifugal force or other phenomena to release CO_2 from the water. At the same time, however, a condensation process should take place on the water droplets in the mixing chamber so that the resulting water also takes part in the subsequent compression of CO_2.

Nevertheless, the final parameters can only be determined after the measurement campaign, as it is not entirely clear how the condensation will affect the nature of the flow. Further conversion of the kinetic

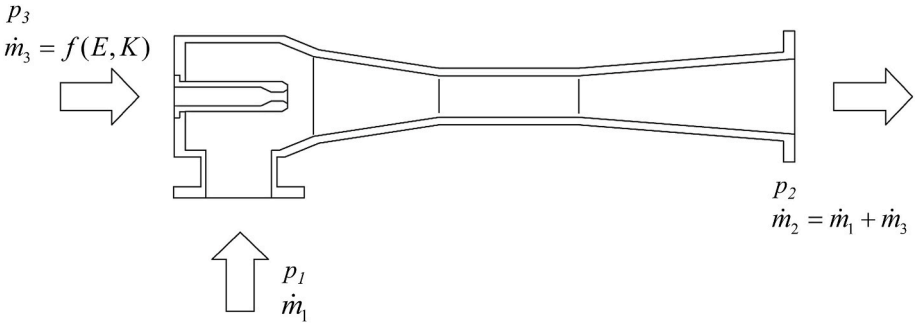

Fig. 4. The scheme of the ejector with marked main parameters: Expansion ratio $E = P_3/P_1$ and the compression ratio $K = P_2/P_1$.

MOST WIEDZY Downloaded from mostwiedzy.pl

Table 1
Spray-Ejector Condenser calculation results (at fixed input data: $p_1 = 0.077$, $p_2 = 1.05$ bar, $t_3 = 15$ °C, $t_1 = 42$ °C).

No.	Motive pressure p_3, bar	Motive water mass flow rate m_3, (kg/s)	Discharge temperature t_2, (°C)	Expansion ratio E, (p_3/p_1)	Compression ratio K, (p_2/p_1)	Mass Entrainment ratio χ, ($\dot{m}_1/\dot{m}_3$)	Volumetric Entrainment ratio χ_V, ($\dot{V}_1/\dot{V}_3$)
1	16.0	11.76	19.5	207.79	13.64	0.0085	143.49
2	15.0	12.13	19.3	194.81	13.64	0.0082	139.08
3	14.0	12.57	19.2	181.82	13.64	0.0080	134.30
4	13.0	13.05	19.0	168.83	13.64	0.0077	129.30
5	12.0	13.60	18.8	155.84	13.64	0.0074	124.07
6	11.0	14.23	18.7	142.86	13.64	0.0070	118.57
7	10.0	14.96	18.5	129.87	13.64	0.0067	112.77
8	9.0	15.82	18.3	116.88	13.64	0.0063	106.62
9	8.0	16.86	18.1	103.90	13.64	0.0059	100.08
10	7.0	18.25	17.8	90.91	13.64	0.0055	92.46
11	6.0	20.09	17.6	77.92	13.64	0.0050	83.98
12	5.0	22.56	17.3	64.94	13.64	0.0044	74.76
13	4.0	26.10	16.9	51.95	13.64	0.0038	64.63

energy of the mixture into its compression energy takes place in the outlet diffuser, where the stream is decelerated. Separation of the components can also occur in the diffuser but ultimately takes place in the separator (*S* in Fig. 1). There should be a substantial increase in outlet pressure to the required value in the diffuser. The diffuser's performance as a flow inhibition device is highly dependent on the homogeneity of the velocity field at the outlet of the mixing chamber. Research on diffusers shows that in diffusers with an opening angle of α∼10o, up to 80% of the compression energy can be recovered [30–32].

3.2. Analysis of spray-ejector condenser performances

To calculate the basic operating conditions and analyze the impact of the main SEC parameters on their performances, the simulations of SEC were conducted using adopted curves from GEA and "Steam Jet Vacuum Pump" model [33]. Single-stage steam jet vacuum pumps achieve a compression ratio K (p_2/p_1) of up to 10 given a sufficiently high expansion ratio of E (p_3/p_1). For higher compression ratios (or lower vacuum), multi-stage vacuum pumps are used, which can be modeled by a series of steam jet vacuum pump units. The presented model (Fig. 4) was modified and adapted to use the motive fluid (water) and condense the suction steam (exhaust gases). The presented approach to simulate two-phase ejectors allows to calculate mass flow of motive fluid $\dot{m}_3$ which is needed for entraining the suction flow $\dot{m}_1$ depends on the conditions (p_1, t_1) of the suction medium as well as on the required outlet pressure p_2. In presented simulation model, the motive water $\dot{m}_3$ depends on the compression ratio K (p_2/p_1) and expansion ratio of E (p_3/p_1), and finally on the pressure value at the inlets (p_1,p_3) and outlet (p_2), and on the suction gas parameters conditions (p_1, t_1). The ejector characteristics were modified to set the mass entrainment ratio as a

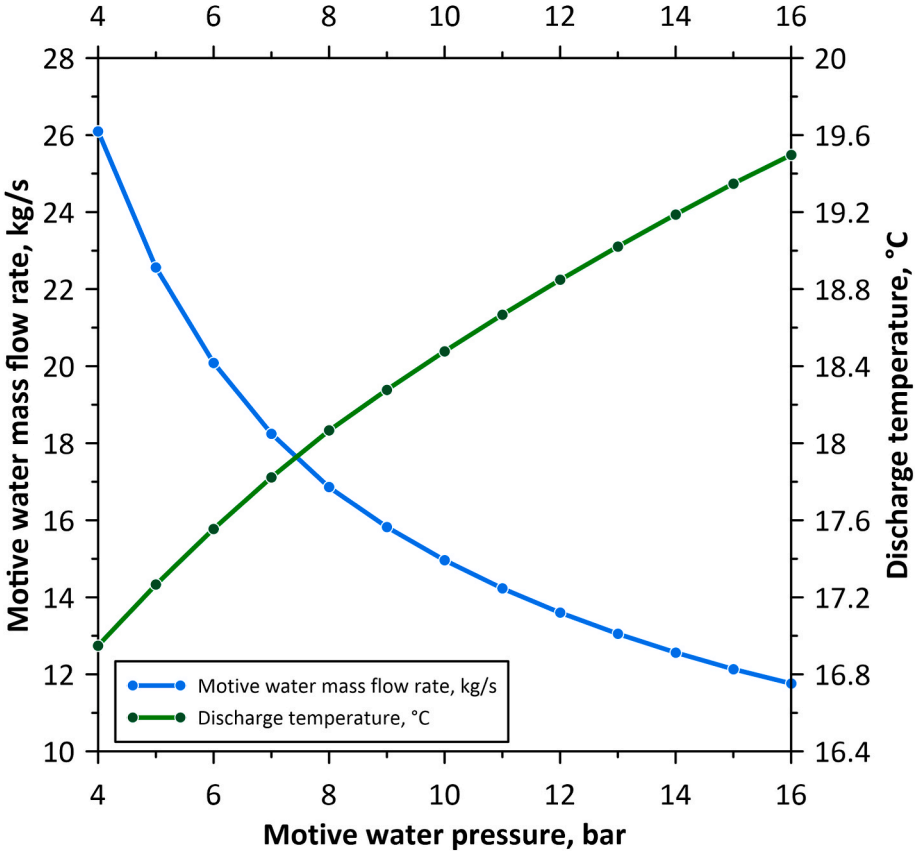

Fig. 5. Motive water mass flow rate m_3 and discharge temperature t_2 as a function of motive water pressure p_3.

MOST WIEDZY Downloaded from mostwiedzy.pl

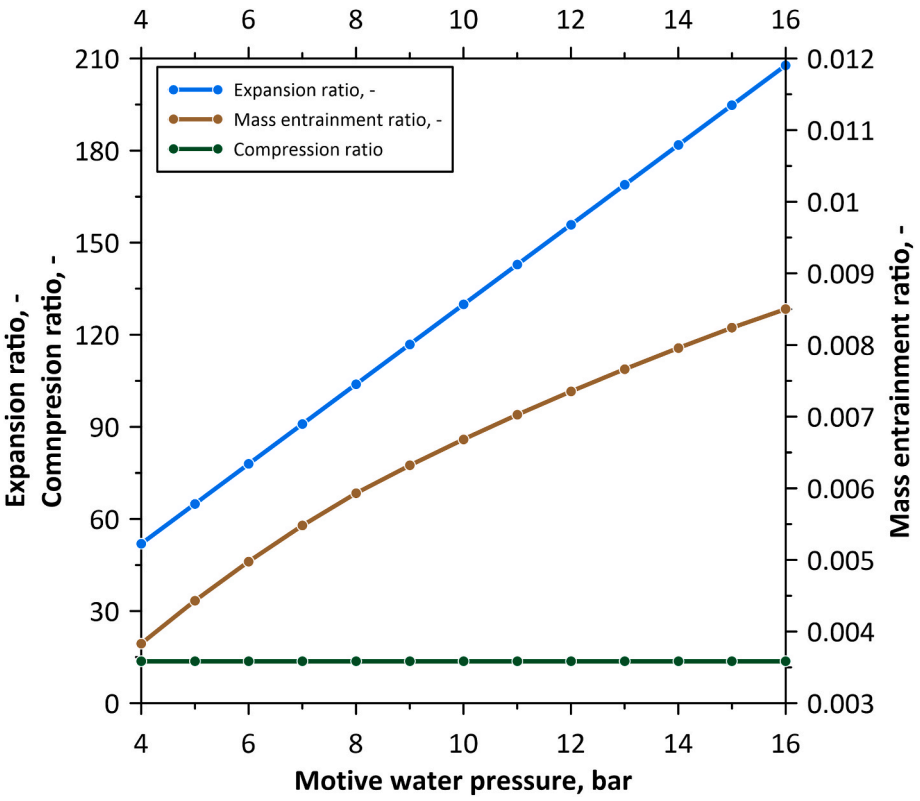

Fig. 6. Expansion ratio E, compression ratio K, and mass entrainment ratio χ as a function of motive pressure p_3.

value in the range between 0.0038 and 0.0059 (0.005 when the motive pressure is equal to 6 bar) [29].

The calculated data as motive water mass flow rate m_3, discharge fluid temperature t_2, expansion ratio E, compression ratio K and mass entrainment ratio χ are presented in Table 1.

$$E = \frac{p_3}{p_1} \tag{1}$$

$$K = \frac{p_2}{p_1} \tag{2}$$

$$\chi = \frac{\dot{m}_1}{\dot{m}_3} \tag{3}$$

where:

p_1, p_2, p_3 - pressure of suction (inlet), discharge (outlet) and motive (inlet) stream, bar

$\dot{m}_1, \dot{m}_2, \dot{m}_3$ - mass flow rate of suction (inlet), discharge (outlet) and motive (inlet) stream, kg/s

The results were computed with the assumption that motive water pressure p_m varies within the range 4–16 bar, motive water temperature t_3 varies within the range 5–35 °C, suction exhaust gas temperature t_1 = 42–162 °C, suction exhaust gas pressure p_1 = 0.077–1.0 bar. Exhaust gas composition was assumed to be xCO2 = 0.18, xH2O = 0.82, and discharge pressure a little above the ambient pressure p_2 = 1.05 bar.

3.2.1. *Impact of motive water pressure and temperature on ejector-condenser operation*

The inlet pressure of motive water to the SEC can vary in the specified range depending on the water pump conditions and can be one of the main parameters to control during the SEC operation. Table 1 shows the results of SEC operation simulation for the case, where the motive pressure in the range 4–16 bar was analyzed using the developed simulation model. The motive pressure value significantly impacts the motive water mass flow rate and mixture outlet temperature, as shown

Table 2
Spray-Ejector Condenser calculation results (at fixed input data: p_1 = 0.077, p_2 = 1.05 bar, p_3 = 6 bar, t_1 = 42 °C).

No.	Motive water temperature t_3 °C	Motive water mass flow rate m_3 (kg/s)	Discharge temperature t_2, (°C)	Expansion ratio E, (p_3/p_1)	Compression ratio K, (p_2/p_1)	Mass Entrainment ratio χ, ($\dot{m}_1/\dot{m}_3$)	Volumetric Entrainment ratio χ_V, ($\dot{V}_1/\dot{V}_3$)
1	35.0	20.09	37.5	77.92	13.64	0.0050	83.55
2	32.5	20.09	35.0	77.92	13.64	0.0050	83.62
3	30.0	20.09	32.5	77.92	13.64	0.0050	83.69
4	27.5	20.09	30.0	77.92	13.64	0.0050	83.75
5	25.0	20.09	27.5	77.92	13.64	0.0050	83.81
6	22.5	20.09	25.0	77.92	13.64	0.0050	83.86
7	20.0	20.09	22.5	77.92	13.64	0.0050	83.90
8	17.5	20.09	20.0	77.92	13.64	0.0050	83.94
9	15.0	20.09	17.6	77.92	13.64	0.0050	83.98
10	12.5	20.09	15.1	77.92	13.64	0.0050	84.01
11	10.0	20.09	12.6	77.92	13.64	0.0050	84.03
12	7.5	20.09	10.1	77.92	13.64	0.0050	84.04
13	5.0	20.09	7.6	77.92	13.64	0.0050	84.05

MOST WIEDZY Downloaded from mostwiedzy.pl

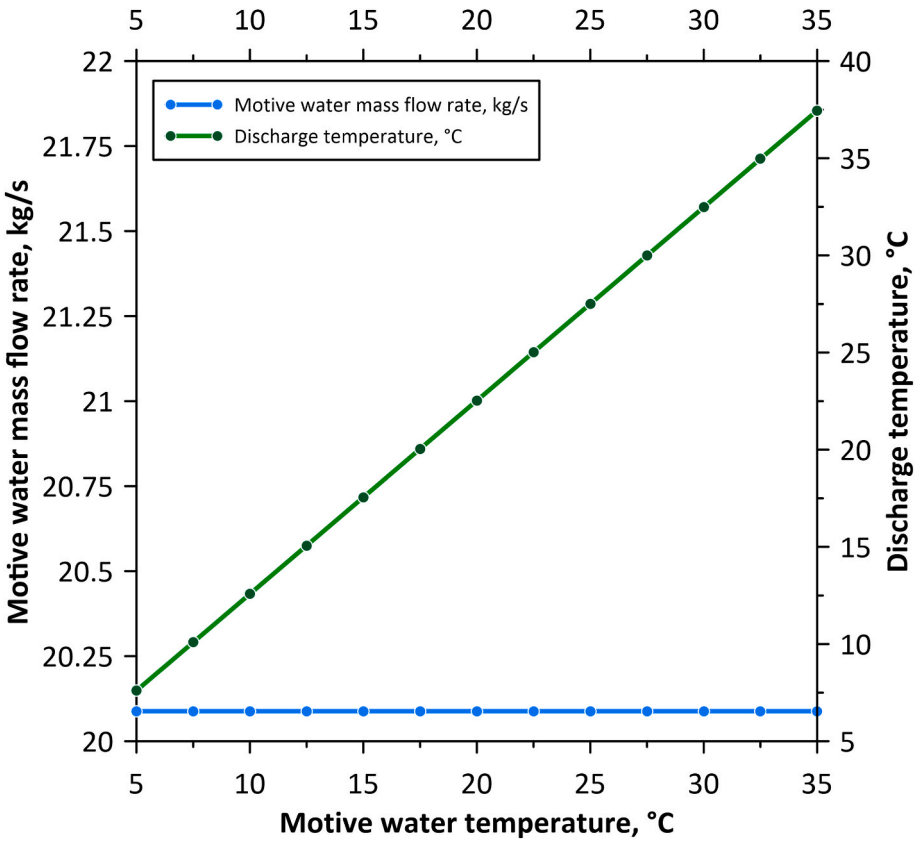

Fig. 7. Cooling water mass flow rate m_3 and discharge temperature t_2 as a function of motive water temperature t_3.

Table 3
Spray-Ejector Condenser calculation results (at fixed input data: $p_1 = 0.077$, $p_2 = 1.05$ bar, $p_3 = 6$ bar, $t_3 = 15$ °C).

No.	Suction temperature t_1, °C	Motive water mass flow rate m_3, (kg/s)	Discharge temperature t_2, (°C)	Expansion ratio E, (p_3/p_1)	Compression ratio K, (p_2/p_1)	Mass Entrainment ratio χ, $(\dot{m}_1/\dot{m}_3)$	Volumetric Entrainment ratio χ_V, $(\dot{V}_1/\dot{V}_3)$
1	162.0	21.89	17.6	77.92	13.64	0.0046	106.43
2	152.0	21.73	17.6	77.92	13.64	0.0046	104.73
3	142.0	21.58	17.6	77.92	13.64	0.0046	103.00
4	132.0	21.42	17.6	77.92	13.64	0.0047	101.24
5	122.0	21.27	17.6	77.92	13.64	0.0047	99.45
6	112.0	21.12	17.6	77.92	13.64	0.0047	97.63
7	102.0	20.97	17.6	77.92	13.64	0.0048	95.77
8	92.0	20.82	17.6	77.92	13.64	0.0048	93.89
9	82.0	20.67	17.6	77.92	13.64	0.0048	91.97
10	72.0	20.52	17.6	77.92	13.64	0.0049	90.02
11	62.0	20.38	17.6	77.92	13.64	0.0049	88.04
12	52.0	20.23	17.6	77.92	13.64	0.0049	86.03
13	42.0	20.09	17.6	77.92	13.64	0.0050	84.05

in Fig. 5.

With increasing motive water pressure, the required mass flow rate of water is lower to keep the same gas pressure at the SEC inlet p_1, which can positively affect the overall cycle efficiency by reducing the power needed for a water pump. The lower mass flow rate of cooling water results in the higher outlet temperature at the SEC outlet t_2,and larger surface area is required of an additional heat exchanger to cool down the mixture of water and CO_2 (*HE2*).

Fig. 6 depicts the impact of motive water pressure on the ejector performance as expansion factor E, compression factor K, and mass entrainment ratio χ. With an increase of inlet water pressure, the compression expansion factor E, volumetric entrainment ratio χ_V, and mass entrainment ratio χ increase from $E = 51.95$, $\chi_V = 64.63$, $\chi = 0.0038$ to $E = 207.79$, $\chi_V = 143.49$, and $\chi = 0.0085$.

The higher motive water inlet temperature only impacts the mixture outlet temperature t_2 (Table 2). The outlet mixture temperature change can be achieved by cooling down the inlet water temperature using a heat exchanger (*HE2*), as presented in Fig. 7. Another reason of the higher outlet temperature is the effectiveness of direct contact condensation inside SEC, but this effect was possible to reproduce using the simulation model presented in the chapter. The analysis using 1D numerical model and 2D CFD models can answer how the outlet temperature t_2, and the presence of non-condensable CO_2 gas reduce direct contact condensation effectiveness inside the SEC.

3.2.2. Impact of exhaust gas pressure and temperature on ejector-condenser operation

Table 3 shows the results of SEC simulation for varied inlet gas mixture temperature t_1. Exhaust gas from the *GT2* outlet are directed to the water heat exchanger *HE1,* and depending on the heat transferred to

MOST WIEDZY Downloaded from mostwiedzy.pl

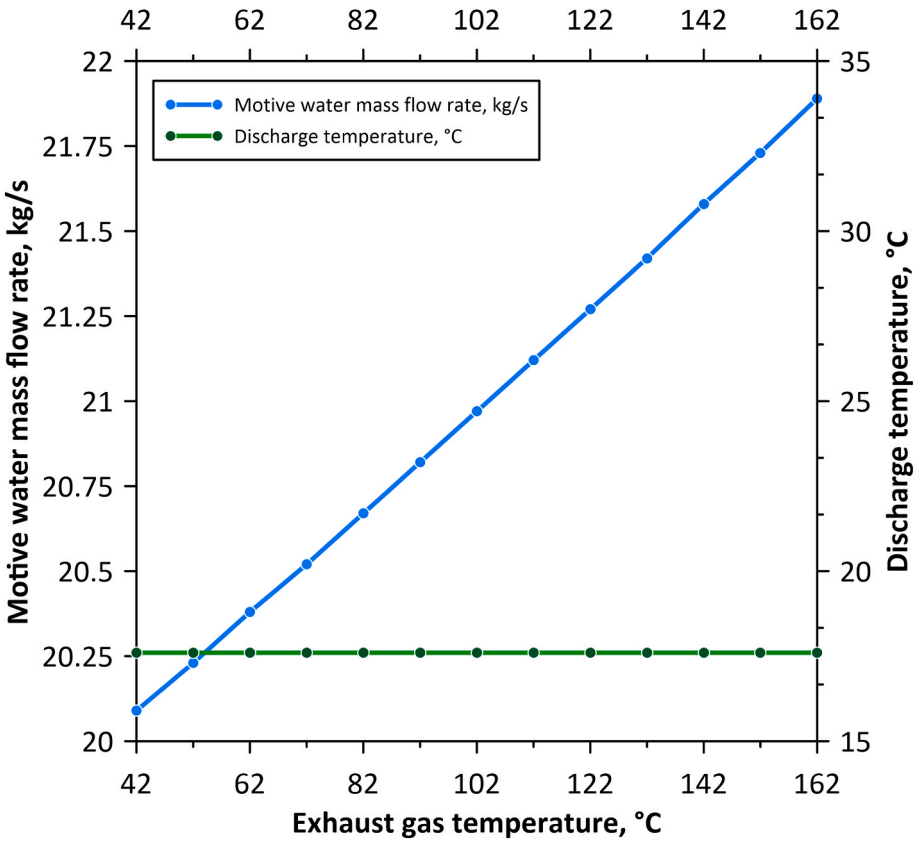

Fig. 8. Cooling water mass flow rate m_3 and discharge temperature t_2 as a function of suction gas temperature t_1.

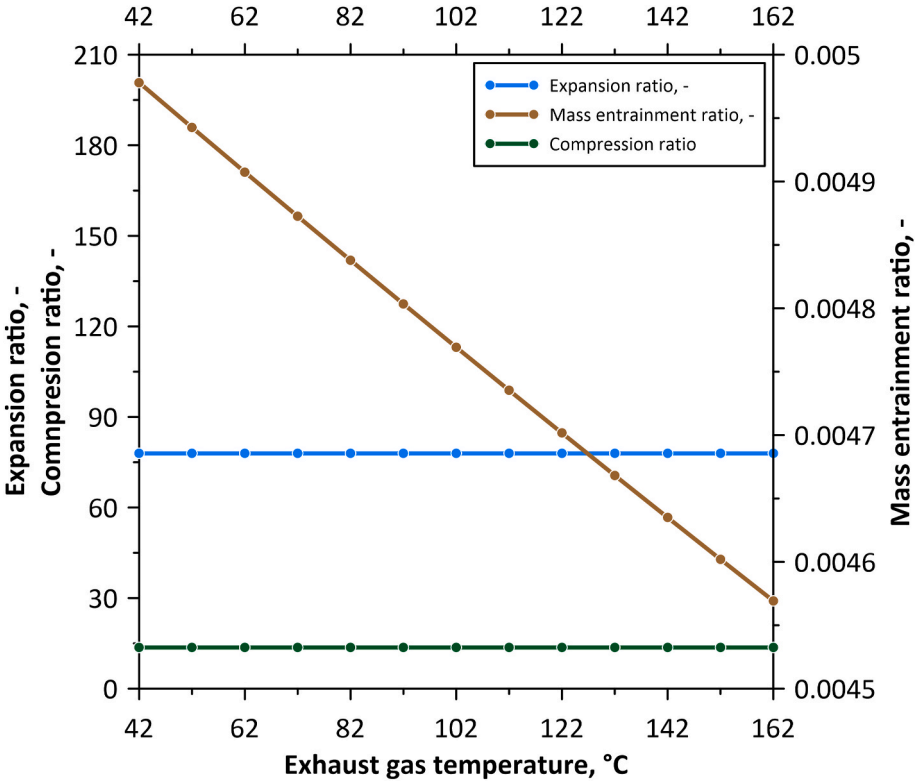

Fig. 9. Expansion ratio E, compression ratio K, and mass entrainment ratio χ as a function suction gas temperature t_1.

MOST WIEDZY Downloaded from mostwiedzy.pl

Table 4
Spray-Ejector Condenser calculation results (at fixed input data: $p_2 = 1.05$ bar, $p_3 = 6$ bar, $t_3 = 15$ °C).

No.	Suction pressure p_1, °C	Motive water mass flow rate m_3, (kg/s)	Discharge temperature t_2, (°C)	Expansion ratio E, (p_3/p_1)	Compression ratio K, (p_2/p_1)	Mass Entrainment ratio χ, ($\dot{m}_1/\dot{m}_3$)	Volumetric Entrainment ratio χ_V, ($\dot{V}_1/\dot{V}_3$)
1	0.8	0.09	98.3	7.50	1.31	1.1276	2469.89
2	0.7	0.14	98.0	8.57	1.50	0.7192	1800.44
3	0.6	0.22	97.3	10.00	1.75	0.4451	1299.83
4	0.5	0.40	94.4	12.00	2.10	0.2471	866.02
5	0.45	0.56	88.0	13.33	2.33	0.1777	692.06
6	0.4	0.80	73.3	15.00	2.63	0.1246	545.93
7	0.35	1.17	57.2	17.14	3.00	0.0852	426.76
8	0.3	1.75	44.2	20.00	3.50	0.0571	333.30
9	0.25	2.80	33.7	24.00	4.20	0.0357	249.98
10	0.2	4.77	26.2	30.00	5.25	0.0210	183.74
11	0.15	8.99	21.0	40.00	7.00	0.0111	129.89
12	0.1	19.60	17.8	60.00	10.50	0.0051	89.42
13	0.077	20.09	17.6	77.92	13.64	0.0050	83.98

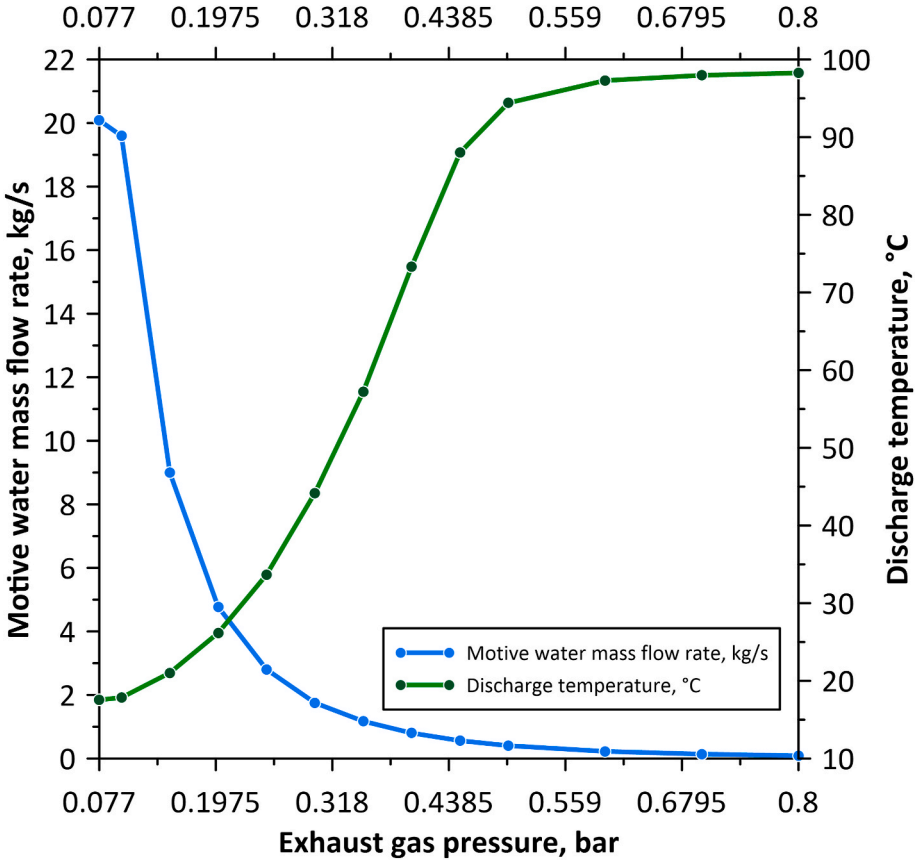

Fig. 10. Cooling water mass flow rate m_3 and discharge temperature t_2 as a function of suction gas pressure p_1.

the water, the inlet gas SEC temperature can change in the range of 42–162° (for the low gas pressure $p_1 = 0.077$ bar). The higher inlet gas temperature requires more cooling water for the SEC, to keep the same constant outlet temperature t_2 (Fig. 8). Mass and volumetric entrainment ratio is reduced where the gas temperature is higher (Fig. 9) and changes in the range of 0.0046–0.005.

The pressure of inlet exhaust gas p_1 depends on the *GT2* outlet conditions, and it is possible to design and maintain during gas turbine operation. Low exhaust gas pressure positively impacts the *GT2* power output and total cycle efficiency, but on the other side, it requires more cooling water, which is presented in Table 4. Decreasing the inlet gas pressure makes the amount of cooling water to the SEC smaller. While reducing the amount of cooling water, keeping the parameters of the sucked gas constant, the outlet temperature of the mixture rises to high values, almost 100 °C (Fig. 10). Although this process can be called flow-

Table 5
Operating conditions for heat balance calculations of SEC.

No.	Parameter	Symbol	Unit	Point (Fig. 4)		
				1	2	3
1	Temperature	t	°C	43	30	15
2	Pressure, bar	p	bar	0.077	1.05	6
3	Mass flow rate	$\dot{m}$	g/s	100	100+ m_2	m_3
4	H_2O mass fraction	x_{H2O}	–	0.82	$x_{CO2,2}$	1
5	CO_2 mass fraction	x_{CO2}	–	0.18	$x_{CO2,2}$	0
6	Enthalpy of H_2O	h_{H2O}	kJ/kg	2579.2	125.7	63.6
7	Enthalpy of CO_2	h_{CO2}	kJ/kg	15.2	4.0	0

MOST WIEDZY Downloaded from mostwiedzy.pl

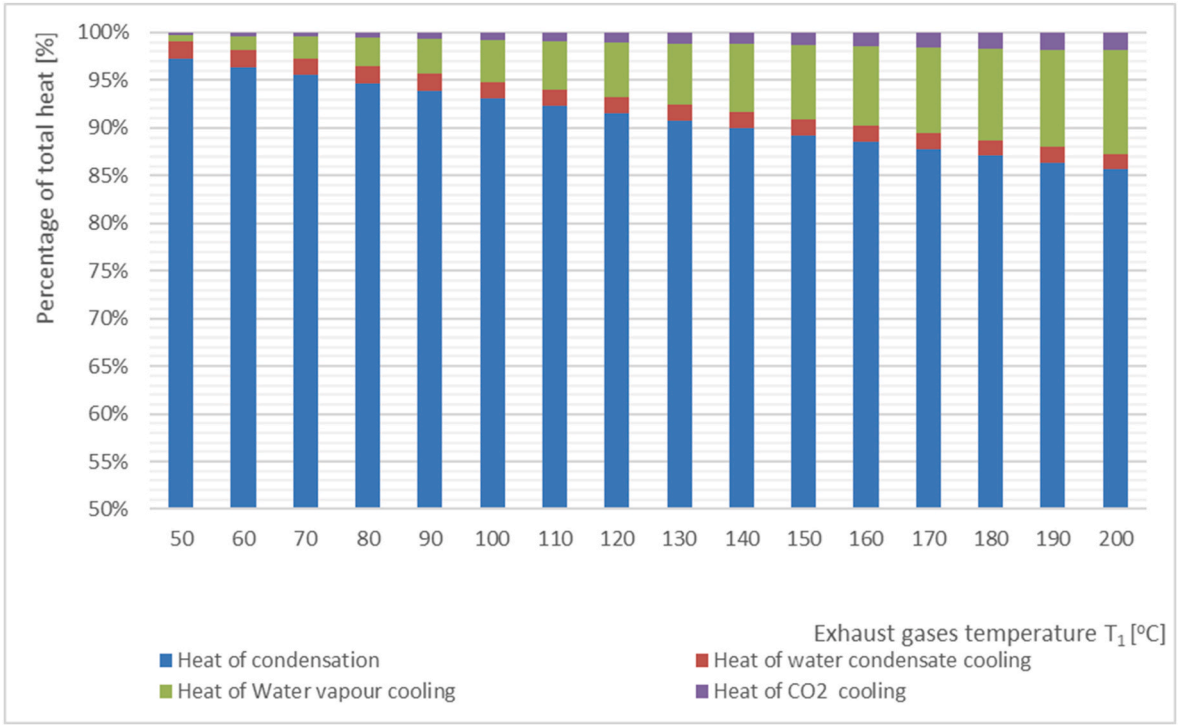

Fig. 11. Share of heat transfer processes in total heat flow rate $\dot{Q}_{eg}$ at different inlet temperatures t_1.

efficient and full condensation is theoretically possible under such conditions, too high a temperature at the SEC outlet is not desirable. Such a process will also be difficult to obtain for designing and constructing a two-phase ejector with such a high mass and volumetric entrainment ratio, as well as considering the problematic heat exchange caused by the presence of CO_2.

3.2.3. *Balance calculations of spray-ejector condenser*

The spray-ejector condenser has two inlets for cooling water and exhaust gases and one outlet for a mixture of water and gases. The boundary conditions for SEC balance calculations are presented in Table 5. The total heat flow rate of exhaust gas cooling is divided into four independent processes: cooling of water vapor, water vapor condensation, cooling of water condensate, and cooling of CO_2. The energy balance for a jet-type flow condenser, assuming perfect condensation and mixing of water and gases, can be presented in the following form:

$$\dot{Q}_{cw} = \dot{Q}_{eg} = \dot{Q}_{vap,cool} + \dot{Q}_{vap,cond} + \dot{Q}_{water,cool} + \dot{Q}_{CO2,cool} \tag{4}$$

where:

$\dot{Q}_{cw}$ - heat flow rate absorbed by the cooling water, W
$\dot{Q}_{eg}$ - heat flow rate transferred from the exhaust gas, W
$\dot{Q}_{vap,cool}$ - heat flow rate of water vapor cooling, W
$\dot{Q}_{vap,cond}$ - heat flow rate of water vapor condensation, W
$\dot{Q}_{water,cool}$ - heat flow rate of condensate cooling, W
$\dot{Q}_{CO2,cool}$ - heat flow rate of CO_2 cooling, W

Heat of water vapor cooling $\dot{Q}_{vap,cool}$ can be calculated using the following relation:

$$\dot{Q}_{vap,cool} = \dot{m}_1 \cdot x_{H2O,1} \cdot \left(h_{h2O,1} - h_{sat,vap}\right) \tag{5}$$

Heat of water vapor condensation is calculated as follows:

$$\dot{Q}_{vap,cond} = \dot{m}_1 \cdot x_{H2O,1} \cdot r \tag{6}$$

Heat of condensate cooling, formed from the water vapor at the SEC gas inlet, can be determined by the following equation:

$$\dot{Q}_{water,cool} = \dot{m}_1 \cdot x_{H2O,1} \cdot \left(h_{sat,liq} - h_{H2O,2}\right) \tag{7}$$

Heat of CO_2 cooling according to the following formula:

$$\dot{Q}_{CO2,cool} = \dot{m}_1 \cdot x_{CO2,1} \cdot \left(h_{CO2,1} - h_{CO2,2}\right) \tag{8}$$

Heat absorbed by the cooling water is calculated using the following relation:

$$\dot{Q}_{CW} = \dot{m}_3 \cdot c_w \cdot (t_2 - t_3) \tag{9}$$

The enthalpy values used in Eqs. (5)–(7), of water vapor and liquid comes from IAPWS-IF-97 steam tables [34], and the enthalpy of carbon dioxide CO_2 used in Eq. (8) from NIST (National Institute of Standards and Technology) tables [35]. When the mixture outlet temperature t_2 is assumed, the required mass flow rate of cooling water can be calculated as follows:

$$\dot{m}_3 = \frac{\dot{Q}_{CW}}{c_w \cdot (t_2 - t_3)} \tag{10}$$

To analyze the heat transfer between inlet gases and cooling water in the spray-ejector condenser, the operating conditions presented in Table 5 were assumed as the nominal operating conditions.

The impact of exhaust gas inlet temperature t_1 on the share of cooling of water vapor $\dot{Q}_{vap,cool}$, water vapor condensation $\dot{Q}_{vap,cond}$, cooling of water condensate $\dot{Q}_{water,cool}$ and cooling of CO_2 $\dot{Q}_{CO2,cool}$ in the total heat flow rate from exhaust gases to cooling water is presented in Fig. 11. Heat flow rate of water condensate cooling to outlet mixture final temperature t_2 is stable because only the inlet exhaust temperature was changed. With increased temperature t_1 the share of water vapor cooling $\dot{Q}_{vap,cool}$ and CO_2 cooling $\dot{Q}_{CO2,cool}$ is also increased, but the share of heat flow rate in this process does not exceed 15%. Heat flow rate of water vapor condensation $\dot{Q}_{vap,cond}$ is a crucial process. The share of heat from CO_2 cooling in total heat does not exceed 3% for the whole analyzed inlet gas temperature range. The amount of cooling water mass flow rate was calculated also using Eq. (10). The linear relationship between the

MOST WIEDZY Downloaded from mostwiedzy.pl

amount of cooling water and exhaust gas temperature t_1 presents the case where the full condensation and perfect mixing of liquid and gas occurs. In that case, the cooling mass flow rate varies in the range from 2.93 to 3.35 kg/s, for inlet gas temperature from 43 °C to 200 °C, respectively. The analyzes presented in the chapter are intended to indicate the directions of development for the development of the SEC, so that the basic geometry can generate appropriate negative pressures, ensuring the best possible condensation in the presence of the inert gas CO_2. The effectiveness of ejector operation and direct contact condensation with non-condensable gas presence requires more advanced analyses using developed numerical models and experimental campaigns.

3.3. Numerical modeling of spray-ejector condenser

The chapter presents the main data for the different numerical and analytical approaches applied to developing new steam direct contact condensation models in the presence of inert CO_2 gas. These approaches allow for modeling the Spray-Ejector Condenser operation, evaluating its efficiency, and preparing the final design of the SEC for the application in the nCO_2PP cycle. The complexity of physical phenomena occurring in the Spray Ejector Condenser (SEC) imposes demanding requirements on the computational tool to be used. In the presented approach of 1D Spray-Ejector Condenser modeling, the original form was developed purely for transonic flows in two-phase CO_2 ejectors and was tuned according to the experimental data registered at the CO_2 test rig at SINTEF Energi laboratory. The tuning procedure comprised basically adjusting the two parameters crucial for capturing the momentum transfer intensity and effectiveness, namely (i) the equivalent roughness of the mixing layer and (ii) the mixing layer drag coefficient [24].

The CFD model of the developed device can be made: two-dimensional flow, axisymmetric, steady-state, liquid–gas multiphase flow, heat transfer mechanism. The model of selected problem includes Reynolds-Averaged Navier-Stokes Turbulence (RANS) model (k-w SST) complex interactions between phases. Multiphase flow regime set in case of liquid-gas interaction, can be described with the following approaches and properties: Drag force (Schiller-Naumann - First and Second Regime Drag Coefficient, Strybelj-Tiselj Intermediate Drag Coefficient), Interaction Area Density (First Regime Interaction Length Scale 0.001 m, Second Regime Interaction Length Scale 0.0005 m), Interaction Length Scale, Interphase Energy Transfer, Large Scale. To model the condensation process, Spalding Evaporation/Condensation model for Mixture Multiphase Model (MMP) can be used in the developed CFD model. The main idea of this model is to express the steady convective mass transfer phenomena using the Ohm's law relation [36, 37]:

$$\dot{m} = gB \tag{11}$$

where:

$\dot{m}$ - rate of the transfer of substance, kg/s

g - surface conductance, kg/s

B - dimensionless driving force

Another approach to condensation process modeling in the developed 2D CFD model is the Boiling/Condensation model, which is also available where the Mixture Multiphase Model (MMP) is used. The model is thermally driven, and the rate of boiling/condensation depends only on the heat transfer rate between phases. The concentration-driven mass transfer is not taken into account. The interface mass flux is calculated based on the formula:

$$g^{(ij)} = \frac{q_i^{(ij)} + q_j^{(ij)}}{\Delta h_{ij}} \tag{12}$$

where:

$g^{(ij)}$– mass transfer flux from phase i to phase j, kg/(m^3·s).

$q_i^{(ij)}$ – heat transfer flux from the interface to i (continuous phase), W/m.^{3}

$q_j^{(ij)}$ – heat transfer flux from the interface to j (dispersed phase), W/m.^{3}

Δh_{ij} – enthalpy difference (latent heat), J/kg

The heat transfer rate from the phase-change interface to each of the two phases can be calculated as follows:

$$q_i^{(ij)} = h_i^{(ij)} \alpha_{ij} \left(T_{ij} - T_i\right) \tag{13}$$

$$q_j^{(ij)} = h_j^{(ij)} \alpha_{ij} \left(T_{ij} - T_j\right) \tag{14}$$

where:

$h_i^{(ij)}$ – heat transfer coefficient, W/(m^2·K).

α_{ij}– weighted coefficient

T_{ij} – interface temperature (saturation temperature), K

T_i, T_j– bulk temperature of continuous/dispersed phase, K

The 2-dimensional, steady-state axisymmetric CFD model of a Spray-Ejector Condenser was developed. The multiphase flow was calculated using the Mixture Multiphase Model (MMP). The turbulence was computed using Realizable k-Epsilon with Two-layer All y + wall treatment model. Boiling/Condensation model, where the condensation rate is calculated based on the heat balance, was assumed. Continuous-dispersed topology was applied to steam-water interaction, where the phase interfacial area was calculated using the average droplet diameter. Steady-state equations of the continuity, momentum, and energy for the Mixture Multiphase Model based on the Euler-Euler, used to model SEC are presented below:

$$\int_A \rho_m \mathbf{v}_m d\mathbf{a} = 0 \tag{15}$$

$$\int_A \rho_m \, \mathbf{v_m} \otimes \mathbf{v_m} \cdot d\mathbf{a} = -\int_A p \, \mathbf{I} \cdot \, d\mathbf{a} + \int_A \mathbf{T}_m \cdot d\mathbf{a} + \int_V \mathbf{f_b} \cdot \, dV \tag{16}$$

$$\int_A \rho_m \, H_m \, \mathbf{v_m} \cdot d\mathbf{a} = -\int_A \dot{\mathbf{q}} \cdot \, d\mathbf{a} + \int_A \mathbf{T}_m \mathbf{v_m} \cdot d\mathbf{a} + \int_V (\mathbf{f_b} \mathbf{v_m} + S_e) \cdot \, dV \tag{17}$$

The transport equation (which occurs for single-fluid models) for volume fractions of i-phase is presented:

$$\int_A \alpha_i \, \mathbf{v_m} \cdot d\mathbf{a} = -\int_A S_{u,i} \cdot \, dV + \int_A \frac{\mu_t}{\sigma_t \rho_m} \nabla \alpha_i + d\mathbf{a} \tag{18}$$

The turbulence was modeled using the k-ω SST turbulence model, which is an eddy viscosity model based on RANS (Reynolds-averaged Navier-Stokes) approach. The equation for the turbulent dynamic viscosity and the transport equations of turbulent kinetic energy k and specific dissipation rate ω are as follows:

$$\mu_t = \rho \, k \, T_t \tag{19}$$

$$\nabla \cdot (\rho k \bar{\mathbf{v}}) = \nabla[(\mu + \sigma_k \mu_t) \nabla k] + P_k - \rho \, \beta^* f_\beta (\omega \, k - \omega_o k_o) + S_k \tag{20}$$

$$\nabla \cdot (\rho \omega \bar{\mathbf{v}}) = \nabla[(\mu + \sigma_\omega \mu_t) \nabla \omega] + P_\omega - \rho \, \beta f_\beta \left(\omega^2 - \omega_0^2\right) + S_\omega \tag{21}$$

In order to maximize the device's efficiency, a proper ejector design and analysis is required. The adiabatic irreversible flow model [14] is used for the ejector analysis, wherein frictional losses through the ejector are considered. The study focuses on the ejector nozzle, pre-mixing chamber, mixing section, and diffuser for the ejector design. Based on literature data, flow properties and ejector geometry are considered using thermodynamic equations, conservation equations, and other assumptions.

MOST WIEDZY Downloaded from mostwiedzy.pl

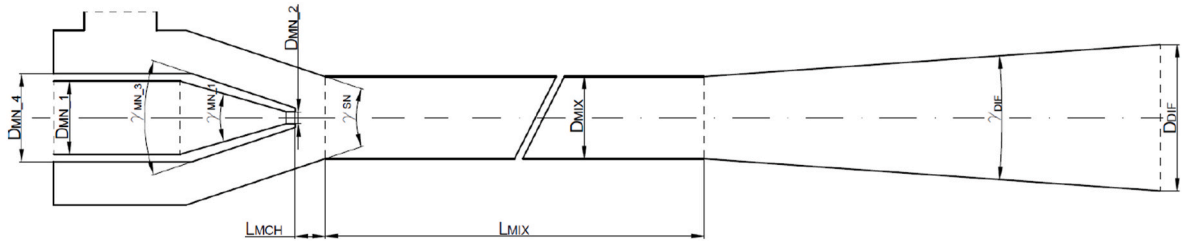

Fig. 12. Two-phase ejector condenser with main dimensions.

Table 6
Boundary conditions imposed for dimensioning of SEC.

Parameter	Motive stream	Suction stream	Outlet
Pressure, bar	12	output	ca. 1 bar
Temperature, deg C	17	150	output
Mass flow rate, kg/s	degree of freedom	0.01	output
Mass fraction of H_2O,-	100%	80%	output

4. Design of spray-ejector condenser based on the simulation and CFD modeling results

The results of the mathematical modeling of the Spray-Ejector Condenser should lead to the development of the basic geometrical design of the proposed solution of the two-phase ejector condenser. The main geometrical parameters allowing to design of the device are presented in Fig. 12.

The initial boundary conditions used for dimensioning of SEC, giving the possibility to install SEC in the developed nCO2pp cycle are listed in Table 6. After analysis of simulations results, and impact of operating conditions on SEC performances the modifications of boundary conditions (temperature, mass flow rate and pressure of exhaust gases, as well as, H_2O/CO_2 ratio at SEC inlet) were made to define the basic design of SEC in tow variants – LPL and HPL.

The data presented in Tables 7 and 8 are the results of the basic design process, obtained thanks to the proposed 1D numerical modeling approach. Two separated variants represent two solutions that should allow high steam condensation efficiency in the presence of inert CO_2 gas. High effective steam condensation occurs with the pressure increase of the mixture at the SEC outlet starting from two different points of exhaust gas pressure, 0.9 (LPL solution) and 0.2 bar (HPL solution), respectively. The mass flow rate of the developed geometrical design of LPL and HPL solution was reduced to 10 g/s of exhaust gases, according to the limitations coming from SEC size.

The calculation of the main properties at the inlets at the outlet for the selected developed variants of SEC (Low-Pressure Lift – LPL; High-Pressure Lift – HPL) compared with the results developed with the use of simulation model (section 3.2) are presented in Table 9. The results presented in Table 9 are the motive water mass flow rate needed to generate low pressure at the suction side (p_1) and to condense steam in direct contact with water. The averaged outlet temperature at the SEC outlet is calculated based on the balance calculations. The expansion ratio E, compression ratio K, and mass entrainment ratio χ are estimated too. More detailed approaches are needed to evaluate SEC performances and investigate physical phenomena inside the SEC during the turbulent flow of water/steam/CO_2 mixture and during the direct contact condensation process.

The results of CFD analysis using the developed CFD model of SEC, shows that various droplet diameter has a strong impact on the Spray-Ejector Condenser inlet pressure and condensation process. The following droplet diameter sizes were investigated: $d = 0.4$ mm, $d = 0.6$ mm, $d = 0.8$ mm, $d = 1$ mm, $d = 1.5$ mm, and $d = 2$ mm. Lower water droplet size at the SEC inlet generates lower exhaust gas inlet pressure and more dynamic growth towards the outlet (Fig. 13, Fig. 14). The greatest pressure increase in pressure is observed in the mixing chamber.

The compression effect of the mixture is visible in all considering cases. The exhaust gas inlet pressure varies from 0.85 bar to 0.98 bar and is dependent on the inlet water droplet diameter. Smaller average droplet diameter generates lower inlet pressure because droplet size affects the water vapor condensation rate and helps create a suction effect. The most significant pressure lift effect, shown in Fig. 14, can be observed in the constant-cross-sectional area mixing chamber for x between 0.1 m and 1.1 m.

Various droplet diameter has an impact on the interfacial area and, thereby, the condensation process. Condensation/boiling mass transfer rate contours for various average droplet diameters is presented in Fig. 15. Smaller droplet sizes ensures a higher condensation mass transfer rate, and the condensation is the most intensive at the beginning of the mixing chamber (Fig. 16). The achieved highest value of condensation transfer rate was nearly 300 kg/(m^3·s) for $d = 0.4$ mm droplet diameter. For $d = 2.0$ and $d = 1.5$ mm droplet diameters, the condensation transfer was one order of magnitude smaller.

The presented results of CFD modeling confirm that the impact of average droplet diameter can be a crucial issue in the case of the direct contact condensation process. It directly affects the interfacial area and, thus, the condensation mass transfer rate. Therefore, the more detailed

Table 7
Main dimensions of the two-phase ejector condenser LPL.

Parameter	Value	Parameter	Value	Parameter	Value	Parameter	Value
D_{MN_1} [mm]	25.4	D_{DIF} [mm]	100	L_{MCH} [mm]	25	γ_{SN} [°]	45
D_{MN_2} [mm]	3	D_{MIX} [mm]	25.4	γ_{MN_1} [°]	30	γ_{DIF} [°]	10
D_{MN_4} [mm]	40	L_{MIX} [mm]	1050	γ_{MN_3} [°]	45		

Table 8
Main dimensions of the two-phase ejector condenser HPL.

Parameter	Value	Parameter	Value	Parameter	Value	Parameter	Value
D_{MN_1} [mm]	50	D_{DIF} [mm]	100	L_{MCH} [mm]	28	γ_{SN} [°]	45
D_{MN_2} [mm]	10.73	D_{MIX} [mm]	50	γ_{MN_1} [°]	30	γ_{DIF} [°]	10
D_{MN_4} [mm]	80	L_{MIX} [mm]	800	γ_{MN_3} [°]	45		

MOST WIEDZY Downloaded from mostwiedzy.pl

Table 9
The basic parameters calculated for the designed installation and selected two SEC variants.

No.	Parameter	Unit	SEC variant			
			HPL-0D	LPL-0D	HPL-1D	LPL-1D
1	Inlet pressure of the steam/CO_2 mixture	bar	0.077	0.9	0.2	0.9
2	Steam mass flow rate of at the inlet	g/s	82	8	8	8
3	CO_2 mass flow rate at the inlet	g/s	18	2	2	2
4	Steam/CO_2 temperature at the inlet	°C	42	146.89	150	150
5	Motive water pressure at the inlet	bar	6	12	12	12
6	Motive water mass flow rate at inlet	g/s	20,088	339	4399	340
7	Motive water temperature at the inlet	°C	15	17	17	17
8	Water, steam and CO_2 mixture mass flow rate at outlet	g/s	20,188	349	4409	350
9	Averaged mixture temperature at the SEC outlet	°C	17.55	32.23	18.4	32.2
10	Expansion ratio	–	77.92	13.33	60	13.33
11	Compression ratio	–	13.63	1.355	5.45	1.25
12	Mass Entrainment Ratio	–	0.00497	0.0286	0.0023	0.0294
13	Volumetric Entrainment Ratio	–	84	55.986	19.62	56.38

modeling results and tuned models should be further used to dimension the SEC to find the best operating conditions. At the same time, a new tuning procedure is expected to be performed once experimental data recorded at the SEC test facility are available. The preliminary results of detailed SEC modeling indicate that full condensation inside the SEC is possible, but the increased CO_2 content in the flue gas strongly reduces condensation efficiency. For the presented cases and the basic developed design of LPL and HPL solution, the condensation efficiency is reduced because of relatively high CO_2 ($x_{CO2} = 20\%$) content at the suction side of SEC. The gas temperature at the SEC outlet varies between 120 and 147 °C, and the water temperature at the outlet can vary between 18 and 30 °C.

5. Conclusions

The difference between surface-type and jet-type condensers is the most important reason for their application. Even if the surface type condensers are more popular and widely used in the power engineering sector, in the analyzed nCO2PP cycle, the application of jet-type condensers is possible because of exhaust gas quality and compositions (H_2O and CO_2). The paper describes the idea of Spray-Ejector Condeser combination with the nCO_2PP cycle in detail. The mass flow rate of

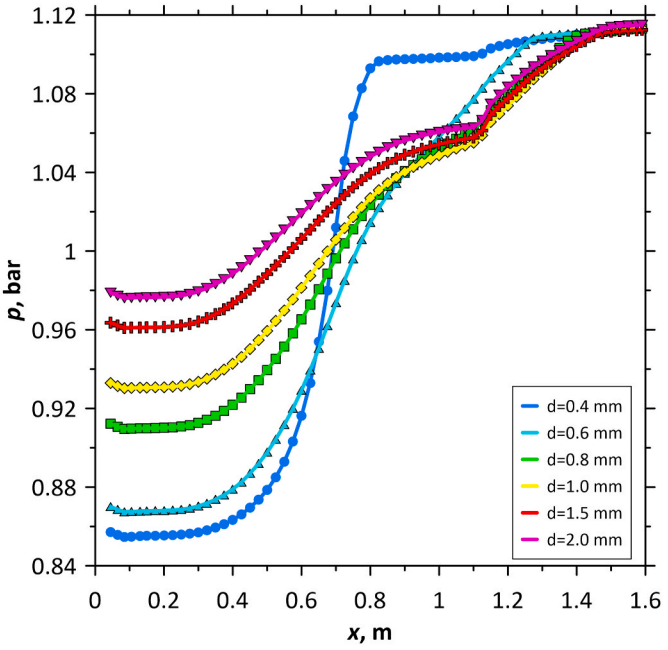

Fig. 14. The change of average static pressure p along the flow inside SEC, for various droplet size d (0.4 mm; 0.6 mm; 0.8 mm; 1 mm; 1.5 mm; 2 mm).

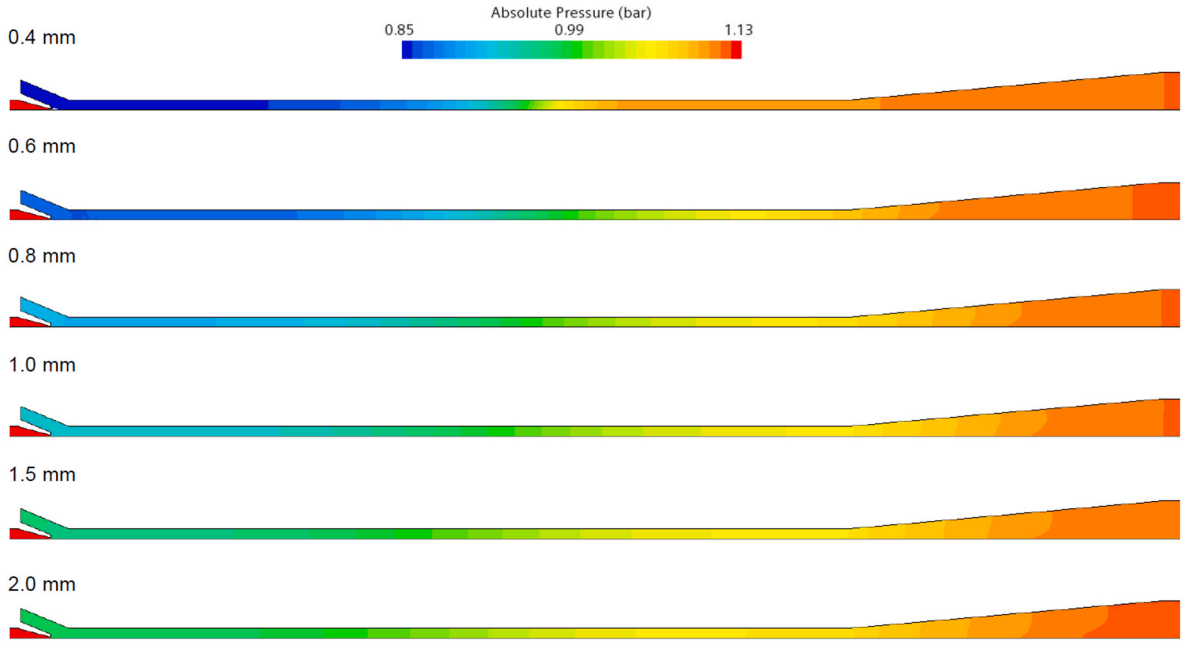

Fig. 13. Static pressure distribution in the Spray-Ejector Condenser for various average droplet diameters.

MOST WIEDZY Downloaded from mostwiedzy.pl

Fig. 15. Boiling/Condensation mass transfer rate field for various droplet size.

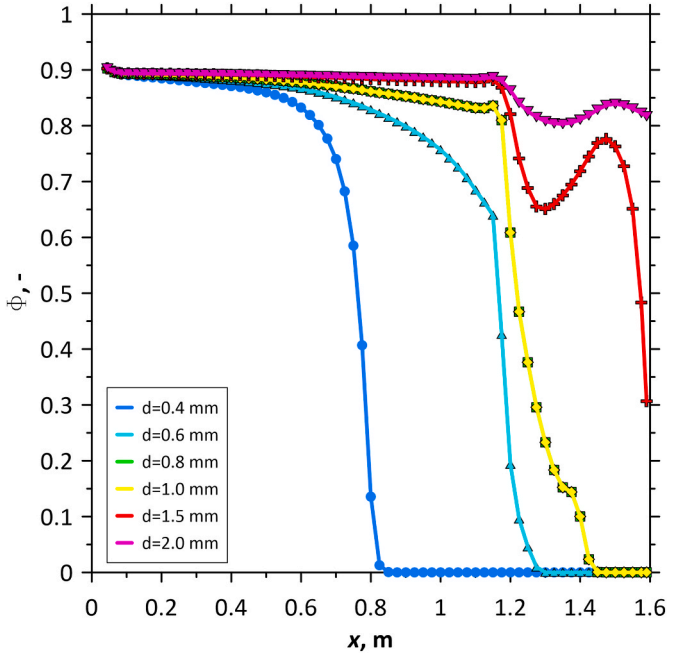

Fig. 16. The change of steam volume fraction φ along the flow inside the SEC, for various droplet size (0.4 mm – grey color; 0.6 mm – yellow color; 0.8 mm – orange color; 1 mm – dark blue color; 1.5 mm – light blue; 2 mm – green color).

motive water strongly depends on ejector design and entrainment fraction ratio (mass/volumetric). In the analyzed cycle, one of the main issues is to design and develop the Spray-Ejector Condenser system to keep the low pressure of exhaust gases. Using the developed simulation model and adopted characteristic curves of ejector operation, the range of the main properties of SEC operation was calculated. Main operating conditions such as motive water mass flow rate, outlet pressure, outlet temperature, expansion ratio, compression ratio, and mass entrainment ratio were estimated. The heat flow rate of water vapor condensation $\dot{Q}_{vap,cond}$ is a crucial process, and for all cases increased 85%. With increased inlet exhaust gas temperature t_1 the share of water vapor cooling $\dot{Q}_{vap,cool}$ and CO_2 cooling $\dot{Q}_{CO2,cool}$ is increased, but the share of heat flow rate in this process does not exceed 15%. Because of that, during the design process of SEC, the inlet exhaust gas temperature was increased from 42 °C to 150 °C. With increasing motive water pressure, the required mass flow rate of water is lower to keep the same gas pressure at the SEC inlet p_1, which can positively affect the overall cycle efficiency by reducing the power needed for a water pump. In the design process using 1D modeling, inlet motive water pressure was assumed two times higher (12 bar instead of 6 bar). The mass flow rate of exhaust gases sucked by SEC was reduced from 100 g/s to 10 g/s because of the high values of motive water mass flow rate needed to condense the steam.

The different modeling approaches, briefly described in the paper and based on the proposed modeling techniques, help develop the basic geometrical design of the Spray-Ejector Condenser. The main dimensional parameters of the basic design are presented. SEC modeling results using different numerical methods allows for analyzing the direct contact condensation inside the SEC and calculating SEC outlet conditions. The CFD modeling results indicate that various droplet diameters strongly impact the gas inlet pressure and gas condensation process inside the mixing chamber. The following 6 different sizes of droplet diameters were investigated: $d = 0.4$ mm, $d = 0.6$ mm, $d = 0.8$ mm, $d = 1$ mm, $d = 1.5$ mm, and $d = 2$ mm. Lower exhaust gas inlet pressure is observed for the cases with smaller inlet droplet diameters. Smaller droplet size also ensure higher condensation mass transfer rate, and the condensation is the most effective. The presented basic design is planned to be tested within experimental activities when the next step of the whole project is connected with experimental verification of selected parameters of Spray-Ejector Condenser modeling results. The experimental activities will be focused on the laboratory scale of the designed installation (steam and CO_2 mass flow rate around 10 g/s), taking into account opportunities to investigate the direct contact condensation process during flow through the two-phase ejector. The measured results can be adopted in the tuning process of developed models and to improve the efficiency of the developed Spray-Ejector Condenser for use in a negative CO2 emission gas power plant.

MOST WIEDZY Downloaded from mostwiedzy.pl

Credit author statement

Paweł Madejski: Conceptualization, Methodology, Software, Validation, Formal analysis, Investigation, Resources, Data curation, Writing-Original draft preparation, Writing-Reviewing and Editing, Visualization, Supervision, Project Administration, Funding Acquisition. Krzysztof Banasiak: Conceptualization, Methodology, Software, Validation, Investigation, Resources, Data curation, Writing-Reviewing and Editing. Paweł Ziółkowski: Conceptualization, Formal analysis, Investigation, Resources, Data curation, Writing-Reviewing and Editing, Project Administration, Funding Acquisition. Dariusz Mikielewicz: Conceptualization, Formal analysis, Investigation, Resources, Data curation, Writing-Reviewing and Editing, Supervision, Project Administration, Funding Acquisition. Jarosław Mikielewicz: Conceptualization, Validation, Investigation, Writing-Reviewing and Editing, Supervision. Tomasz Kuś: Methodology, Software, Validation, Investigation, Data curation, Writing-Original draft preparation, Visualization. Michał Karch: Validation, Investigation. Piotr Michalak: Validation, Investigation. Milad Amiri: Investigation. Paweł Dąbrowski: Investigation. Kamil Stasiak: Investigation. Navaneethan Subramanian: Investigation. Tomasz Ochrymiuk: Investigation, Project Administration, Funding Acquisition.

Declaration of competing interest

The authors declare that they have no known competing financial interests or personal relationships that could have appeared to influence the work reported in this paper.

Data availability

Data will be made available on request.

Ackowledgments

The research leading to these results has received funding from the Norway Grants 2014–2021 via the National Center for Research and Development. Work has been prepared within the frame of the project: “Negative CO2 emission gas power plant” - NOR/POLNORCCS/NEGATIVE-CO2-PP/0009/2019–00 which is co-financed by programme “Applied research” under the Norwegian Financial Mechanisms 2014–2021 POLNOR CCS 2019 - Development of CO2 capture solutions integrated in power and industry processes.

References

[1] Parves M., Steam condenser, Al Falah Univeristy, chapter: Steam turbines and condensers.
[2] Kakaç S, Liu H. Heat exchangers: selection, rating, and thermal design. CRC Press; 2002.
[3] Minkowycz WJ, Sparrow EM, Abraham JP, Gorman JM, editors. Advances in numerical heat transfer. Numerical simulation of heat exchangers, vol. 5. CRC Press/Taylor & Francis Group; 2017.
[4] Kitto JB, Stultz SC. Steam its generation and use. Ohio USA: The Babcock & Wilcox Company; 2005.
[5] Boehm RF, Kreith F. Direct-contact heat transfer processes. In: Kreith F, Boehm RF, editors. Direct-contact heat transfer. Berlin, Heidelberg: Springer; 1988. https://doi.org/10.1007/978-3-662-30182-1_1.
[6] Madejski P, Kuś T, Michalak P, Karch M, Subramanian N. Direct contact condensers: a comprehensive review of experimental and numerical investigations on direct-contact condensation. Energies 2022;15:9312.
[7] Barabash P, Solomakha A, Sereda V. Experimental investigation of heat and mass transfer characteristics in direct contact exchanger. Int J Heat Mass Tran 2020;162:120359.
[8] Zhao X, Fu L, Sun T, Wang JY, Wang XY. The recovery of waste heat of flue gas from gas boilers. Sci. Technol. Built Environ. 2017;23:490–9.
[9] Prananto LA, Juangsa FB, Iqbal RM, Aziz M, Soelaiman TAF. Dry steam cycle application for excess steam utilization: kamojang geothermal power plant case study. Renew Energy 2018;117:157–65.
[10] Sanopoulos D, Karabelas A. H2 abatement in geothermal plants: evaluation of process alternatives. Energy Sources 1997;19:63–77.
[11] Liu D, Jin J, Gao M, Xiong Z, Stanger R, Wall T. A comparative study on the design of direct contact condenser for air and oxy-fuel combustion flue gas based on Callide Oxy-fuel Project. Int J Greenh Gas Control 2018;75(August):74–84.
[12] Ghazwani HA, Khan A, Taranenko PA, Sinitsin VV, Ghazwani MHH, Alnujaie AH, Sanaullah K, Ullah A, Rigit ARH. Hydrodynamics of direct contact condensation process in desuperheater. Fluid 2022;7:313.
[13] Sokolow JJ, Zinger NM. Jet devices. WNT; 1960.
[14] Mikielewicz D, Amiri M, Mikielewicz J. Direct-contact condensation from vapour-gas mixture in a spray ejector condenser for negative CO2 power plant. Gothenburg. In: Conference proceedings, 2nd international conference on negative CO2 emissions; June 14-17, 2022. Sweden.
[15] He S, Li Y, Wang RZ. Progress of mathematical modelling on ejectors. Renew Sustain Energy Rev 2009;13:1760–80.
[16] Colarossi M, Trask N, Schmidt DP, Bergander MJ. Multidimensional modeling of condensing two-phase ejector flow. Int J Refrig 2012;35:290–9.
[17] Ameur K, Aidoun Z, Ouzzane M. Modeling and numerical approach for the design and operation of two-phase ejectors. Appl Therm Eng 2016;109:809–18.
[18] https://nco2pp.mech.pg.gda.pl/pl.
[19] Ziółkowski P, Badur J, Pawlak-Kruczek H, Niedzwiecki L, Kowal M, Krochmalny K. A novel concept of negative CO2 emission power plant for utilization of sewage sludge. In: Proceedings of the 6th international conference on contemporary problems of thermal engineering CPOTE 2020. Gliwice, Poland; 21–24 September 2020. p. 531–42.
[20] Ziółkowski P, Madejski P, Amiri M, Kuś T, Stasiak K, Subramanian N, Pawlak-Kruczek H, Badur J, Niedźwiecki Ł, Mikielewicz D. Thermodynamic analysis of negative CO2 emission power plant using aspen Plus, aspen Hysys, and Ebsilon software. Energies 2021;14:6304. https://doi.org/10.3390/en14196304.
[21] Ziółkowski P, Głuch S, Ziółkowski PJ, Badur J. Compact high efficiency and zero-emission gas-fired power plant with oxy-combustion and carbon capture. Energies 2022;15:2590. https://doi.org/10.3390/en15072590.
[22] Madejski P, Ertesvåg IS, Ziółkowski P, Mikielewicz D. Energy and exergy analysis of negative CO2 emission gas power plant operation using thermodynamic modelling results of the cycle. Gothenburg. In: Conference proceedings, 2nd international conference on negative CO2 emissions; June 14-¬17, 2022. Sweden.
[23] Ertesvåg IS, Madejski P, Ziółkowski P, Mikielewicz D. Exergy analysis of a negative CO2 emission gas power plant based on water-injected oxy-combustion of syngas from sewage sludge gasification and CCS. Energy 2023;278:127690.
[24] Banasiak K, Hafner A. 1D computational model of a two-phase R744 ejector for expansion work recovery. Int J Therm Sci 2011;50(11):2235–47.
[25] SIEMENS Simcenter STAR-CCM+. Software documentation. 2020. 2, Version.
[26] Kuś T, Madejski P. Analysis of turbulent multiphase flow modeling methods in ejector-condenser system, XIV Multiphase Workshop and Summer School, Koszałkowo–Wieżyca k/Gdańska, 2–4.09.2021, book of abstracts. 2021. Gdańsk.
[27] Madejski P, Kuś T, Subramanian N, Karch M, Michalak P. The possibilities of carrying out numerical and experimental tests of jet type flow condensers for application in energy technologies, Wdzydzeanum workshop on Fluid-solid interaction. Gdańsk: books of abstract; 2021.
[28] Madejski P, Michalak P, Karch M, Kuś T, Banasiak K. Monitoring of thermal and flow processes in the two-phase spray-ejector condenser for thermal power plant applications. Energies 2022;15:7151.
[29] Goliński J, Jesionek KJ. Air-steam power plants. IMP PAN; 2009.
[30] Neve R. Diffuser performance in two-phase jet pumps. Int J Multiphas Flow 1991;17:267–72.
[31] Sarevski VN, Sarevski MN. Characteristics of R718 refrigeration/heat pump systems with two-phase ejectors. Int. J. Refrigeration 2016;70:13–32.
[32] Goliński J, Troskolański A. Strumienice teoria i konstrukcja. Warszawa: WNT; 1979.
[33] Steag Energy Services. Ebsilon®Professional, version 15.00. https://www.ebsilon.com/.
[34] Wagner W, Kretzschmar HJ. International steam tables. Properties of water and steam based on the industrial formulation IAPWS-IF97: tables, algorithms, diagrams. Berlin Heidelberg: Springer-Verlag; 2002. Germany.
[35] National Institute of Standards and Technology. Carbon dioxide tables. . [Accessed 9 September 2022]. https://webbook.nist.gov/cgi/inchi/InChI%3D1S/CO2/c2-1-3.
[36] Spalding DB. A standard formulation of the steady convective mass transfer problem. Int J Heat Mass Tran 1960;1:192–207.
[37] Kuś T, Madejski P. CFD modeling of the multiphase flow with condensation in the two-phase ejector condenser. Warsaw: Proc. 7th International Conference on Contemporary Problems of Thermal Engineering; 2022. p. 833–44.

MOST WIEDZY Downloaded from mostwiedzy.pl